*CORROSION SCIENCE AND TECHNOLOGY, Vol.17, No.3(2018), pp.91~100*
[Research Paper]
pISSN: 1598-6462 / eISSN: 2288-6524
DOI: https://doi.org/10.14773/cst.2018.17.3.91

# Anticorrosion Coatings Obtained by Plasma Electrolytic Oxidation on Implant Metals and Alloys

**S. L. Sinebryukhov[1,2,†], S. V. Gnedenkov[1,2], O. A. Khrisanfova[1], A. V. Puz'[1], V. S. Egorkin[1], and A. G. Zavidnaya[1]**

[1]*Institute of Chemistry, Far Eastern Branch, Russian Academy of Sciences, Vladivostok, Russia*
[2]*Far Eastern State Federal University, Vladivostok, Russia*

(Received February 19, 2018; Revised April 29, 2018; Accepted April 30, 2018)

Development of biodegradable implants for treatment of complex bone fractures has recently become one of the priority areas in biomedical materials research. Multifunctional corrosion resistant and bioactive coatings containing hydroxyapatite $Ca_{10}(PO_4)_6(OH)_2$ and magnesium oxide MgO were obtained on Mg-Mn-Ce magnesium alloy by plasma electrolytic oxidation. The phase and elemental composition, morphology, and anticorrosion properties of the coatings were investigated by scanning electron microscopy, energy dispersive spectroscopy, potentiodynamic polarization, and electrochemical impedance spectroscopy. The PEO-layers were post-treated using superdispersed polytetrafluoroethylene powder. The duplex treatment considerably reduced the corrosion rate (>4 orders of magnitude) of the magnesium alloy. The use of composite coatings in inducing bioactivity and controlling the corrosion degradation of resorbable Mg implants are considered promising. We also applied the plasma electrolytic oxidation method for the formation of the composite bioinert coatings on the titanium nickelide surface in order to improve its electrochemical properties and to change the morphological structure. It was shown that formed coatings significantly reduced the quantity of nickel ions released into the organism.

***Keywords:*** *Implant alloys, Protective coating, Plasma electrolytic oxidation, Titanium nickelide*

## 1. Introduction

Development of biodegradable implants for treatment of complex bone fractures has recently become one of the priority areas in biomedical materials research. The overall aim of such development is the exception of the secondary surgery in order to remove temporary implants. The biodegradable implant is supposed to be gradually resorbed by the body during the bone regeneration period (typically 12–14 weeks), causing no adverse effects to the human organism. The implant material should therefore be capable of being dissolved at a slow rate in the chloride-containing physiological environment, forming soluble corrosion products that can be naturally removed from the organism [1–3].

Increased attention has recently been paid to magnesium alloys, which can be used as a material for biodegradable implants. The major advantages of these materials are biocompatibility and suitable mechanical properties, such as a low density and Young's modulus, which are comparable with those of the cortical bone [4,5]. Moreover, anodic dissolution of Mg yields $Mg^{2+}$ cations that are generally non-toxic and cause no adverse side effects. However, extremely high corrosion activity of Mg in chloride-containing environments may result to a premature loss of implant's mechanical strength and a poor cell adhesion and hindered formation of the new bone tissue due to increased alkalinity of the environment. These two factors severely restrict the use of magnesium alloys as a biodegradable material.

Corrosion rate of magnesium may be reduced by alloying and application of protective coatings. Alloying with Al, Zn, Mn, Zr, Ca and rare earths (including Ce) is known to have positive effects on corrosion resistance [6] as well as on mechanical properties of magnesium, which would otherwise have insufficient strength for high-loaded implants manufacturing [7]. Small amounts of Mn, Ca and Zn, which are not foreign to the body, can be tolerated [7], however excessive alloying with some other elements, e.g. Al, could lead to various adverse effects, limiting capabilities of the metallurgical route. This makes the use of anticorrosion coatings on low-alloyed magnesium imminent.

For resorbable Mg implants it is essential that the new

† Corresponding author: sls@ich.dvo.ru

bone tissue growth does not lag behind implant's dissolution [8]. The anticorrosion coating should therefore possess a certain bioactivity, i.e. accelerate bone regeneration along with inhibiting implant corrosion, thus promoting its gradual replacement with bone tissue. Development of such multifunctional coatings, that are both corrosion resistant and bioactive, is vital for resorbable Mg-alloy implants. In this context, bioactive coatings containing native to the bone tissue calcium phosphates are of great interest. New methods for fabrication of calcium phosphate were developed recently for bio-application [9–11]. In particular, synthesis of hydroxyapatite (HA) presented in composition of the coating with appropriate morphology would provide the Mg-alloy surface with required corrosion resistance and bioactivity.

Deposition of calcium phosphate films on Mg alloys has been previously reported using biomimetic [12–14] and sol-gel [15] techniques that are tedious, delicate and multistep procedures, involving complex organic substances and requiring careful control. In contrast, Plasma Electrolytic Oxidation (PEO) is simple and technologically efficient method for surface modification of lightweight metals, including those used for biomedical purposes. PEO-coatings possess a many useful properties such as a strength, hardness and high adhesion to the substrate. Due to the developed surface, PEO-layer may be used as a basis for a composite coating formation. Bioactive HA coatings have been previously formed by PEO on titanium implants [16,17], however the information on HA deposition on Mg is rather limited. Porous PEO-coatings containing amorphous Ca and P compounds were fabricated on Mg alloys in complex calcium hypophosphite and hydroxide based electrolytes [18,19]. These however offered only limited corrosion protection and bioactivity. At the same time, PEO-coatings obtained from silicate–fluoride electrolytes demonstrated high corrosion resistance [20] but no successful attempts was recorded on co-deposition of calcium phosphates by such treatments.

In this work a method is proposed for plasma electrolytic synthesis of calcium phosphate compounds on the surface of Mg-Mn-Ce magnesium alloy. The morphology, elemental and phase composition, corrosion properties of coatings were studied. These hydroxyapatite-containing PEO-layers will ensure the biological activity of the implant with the bone tissue and will reduce the corrosion rate as compared to that of the uncoated metal implant; thus helping to find the solution to the problem of using magnesium implants in medicine.

## 2. Results and discussion

### 2.1. Composite hydroxyapatite-PTFE coatings on Mg-Mn-Ce magnesium alloy

The PEO layers were obtained in electrolyte containing calcium glycerophosphate, sodium fluoride and sodium hydroxide on the MA8 magnesium alloy. These coatings were found to consist of crystalline magnesium oxide and hydroxyapatite phases as well as an amorphous constituent. According to the cross-sectional analysis, the coating thickness is equal to about 60 μm. The coating surface has a highly convoluted heterogeneous relief (Fig. 1a). Pores and cracks typically appear as results of the high pressure and temperatures that realized in the plasma channels during the plasma electrolytic oxidation process [20–23]. Along with the dark areas the film is dense and uniform (Fig. 1b), there are light globular particles, having complex volume form (Fig. 1c), as well as outgrowths, cavities, and pores. In spite of heterogenic morphology and presence of pores and cracks (Fig. 1a) on the surface, this coating has a good adhesion to substrate. According to scratch test results, the critical load for such coating is equal to 22.8 ± 1.5 N.

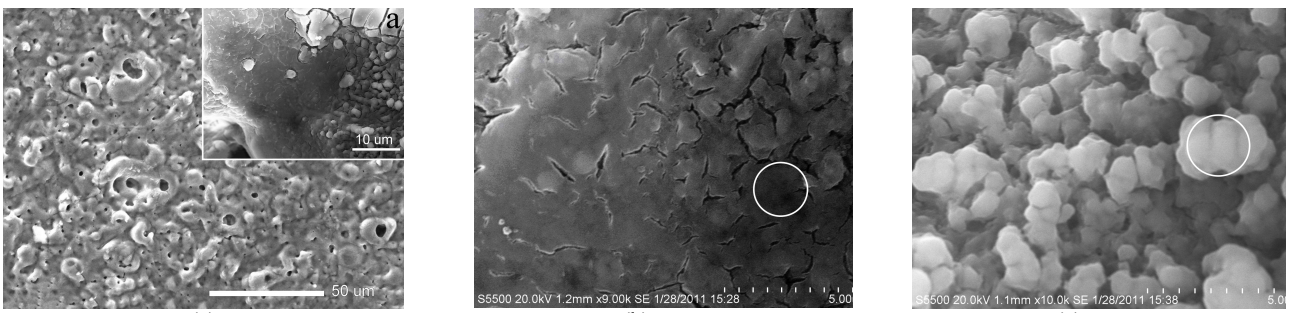


(a) (b) (c)

**Fig. 1 Surface SEM images of the PEO coating on Mg-Mn-Ce magnesium alloy: (a) general view of the coating; (b) dark region; (c) light region.**

**Table 1 Elemental and phase composition of the coatings fabricated on the Mg alloy**

| Area under consideration | Elemental composition (at%) | | | | | | | | Phase composition |
|---|---|---|---|---|---|---|---|---|---|
| | Ca | P | Mg | Na | O | C | F | Ca/P | |
| Light | 14.2 | 8.8 | 2.4 | 4.6 | 38.6 | 19.5 | 11.9 | 1.61 | $Ca_{10}(PO_4)_6(OH)_2$ amorphous phase |
| Dark | 6.6 | 8.7 | 8.3 | 0.8 | 33.0 | 35.6 | 7.0 | 0.76 | MgO |

The elemental analysis attested to the fact that the coatings contain such elements as Ca, P, Mg, Na, O, C, and F (Table 1). The calcium content is higher in the light regions of the PEO coating than in the dark regions, whereas magnesium content follows the opposite trend, indicating that the light regions contained a smaller amount of magnesium oxide. According to Table 1, the Ca/P ratio in the light coating regions of the coating is equal to 1.61, this value is close to that in the bone tissue (1.67). At the same time, calcium content in the dark regions of the coatings is twice as low, with the Ca/P ratio being only 0.76, whereas the magnesium content is higher. These regions appear to be depleted in calcium and consist mostly of MgO. According to Sun, *et al* [24], the formation of a binary compound consisting of sodium and magnesium fluorides $NaMgF_3$ in an amorphous form is also possible in both light and dark regions of the coating.

The presence of carbon in the coating can be attributed to the organic components of the electrolyte (namely, calcium glycerophosphate) that were adsorbed on the surface and/or failed to combust in discharge channels during the PEO process. Organic radicals facilitate longer-lasting discharges, which result in high-temperature synthesis of crystalline compounds (in this case, hydroxyapatite) in the coating [22]. For this reason, an increased content of $Ca_{10}(PO_4)_6(OH)_2$ was observed in light regions, where the carbon content was a lower than if dark regions. Maximum of calcium and phosphorus concentrations in accordance with EDS data obtained on the cross-section have been ascertained in the outer part of coating, while the inner part attached to substrate consists of Mg, O and F. The composition of this part of coatings formed in the fluoride-containing electrolytes consists predominantly of MgO and low content of amorphous $MgF_2$ [20,23]. According to the results of both *in vitro* and *in vivo* experiments [16], hydroxyapatite-containing PEO-coatings fabricated on titanium alloys exhibit high biological activity, considerably accelerating the growth of the bone tissue on the implant surface.

The electrochemical properties were investigated via the potentiodynamic polarization and electrochemical impedance spectroscopy using a 12558WB electrochemical system (Solartron Analytical, England). The measurements were performed in a three-electrode cell in 3 % NaCl solution at room temperature. Platinized niobium grid was used as a counter electrode. The silver-chloride electrode filled with the saturated KCl solution was used as a reference electrode. Prior to the electrochemical measurements, the specimens were kept in the electrolyte for 15 min to let the free corrosion potential $E_C$ be reached.

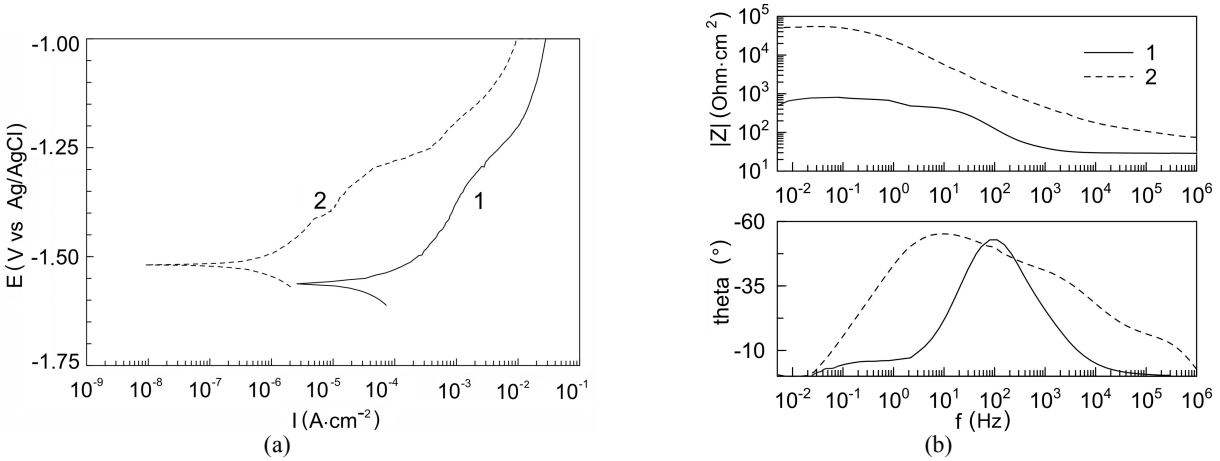


**Fig. 2 Polarisation curves (a) and impedance spectra (b) recorded in a 3 % NaCl solution for the magnesium alloy specimens: (1) uncoated; (2) with PEO-coating.**

**Table 2 Characteristics of corrosion resistance of the studied specimens in 3 % NaCl solution at 20 ºC**

| Sample | $E_C$ (V vs Ag/AgCl) | $I_C$ (A/cm$^2$) | $R_p$ (Ω·cm$^2$) | $\|Z\|_{f\to 0\ \mathrm{Hz}}$ (Ω·cm$^2$) |
|---|---|---|---|---|
| Uncoated | –1.56 | $5.1\cdot10^{-5}$ | $4.9\cdot10^{2}$ | $8.1\cdot10^{2}$ |
| PEO | –1.52 | $1.2\cdot10^{-6}$ | $2.7\cdot10^{4}$ | $5.1\cdot10^{4}$ |

**Table 3 Corrosion properties of the samples in Hank's solution at 37 ºC**

| Sample | $E_C$ (V vs Ag/AgCl) | $I_C$ (A/cm$^2$) | $R_p$ (Ω·cm$^2$) | $\|Z\|_{f\to 0\ \mathrm{Hz}}$ (Ω·cm$^2$) |
|---|---|---|---|---|
| Uncoated | -1.54 | $2.0\cdot10^{-6}$ | $1.3\cdot10^{4}$ | $1.3\cdot10^{4}$ |
| PEO | -1.61 | $1.3\cdot10^{-6}$ | $2.5\cdot10^{4}$ | $3.6\cdot10^{4}$ |
| PEO+SPTFE | -1.50 | $5.4\cdot10^{-9}$ | $1.0\cdot10^{7}$ | $1.9\cdot10^{7}$ |

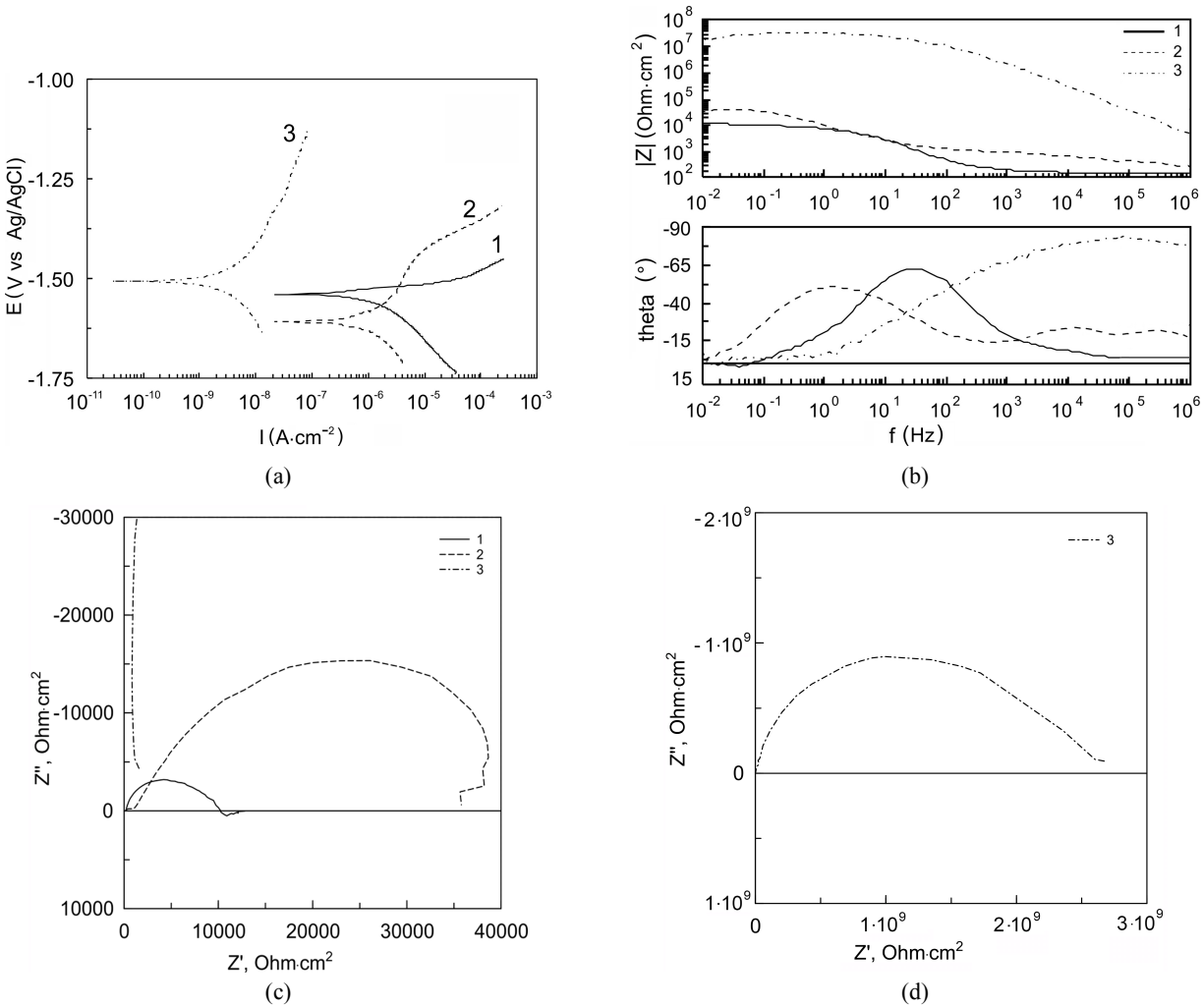


**Fig. 3 Polarization curves (a) and impedance spectra in Bode (b) and Nyquist (c, d) plot recorded in a Hank's balanced salt solution at 37 ºC for the MA8 magnesium alloy specimens: (1) uncoated; (2) PEO-coating; (3) PEO-coating treated with SPTFE.**

The polarization curves were recorded at a potential scan rate of 1 mV/s. The samples were anodically polarized, starting at the potential $E = E_C - 30$ mV.

The corrosion current density, $I_C$, and polarization resistance, $R_p$, were calculated using the Stern-Geary equation. When impedance measurements were carried

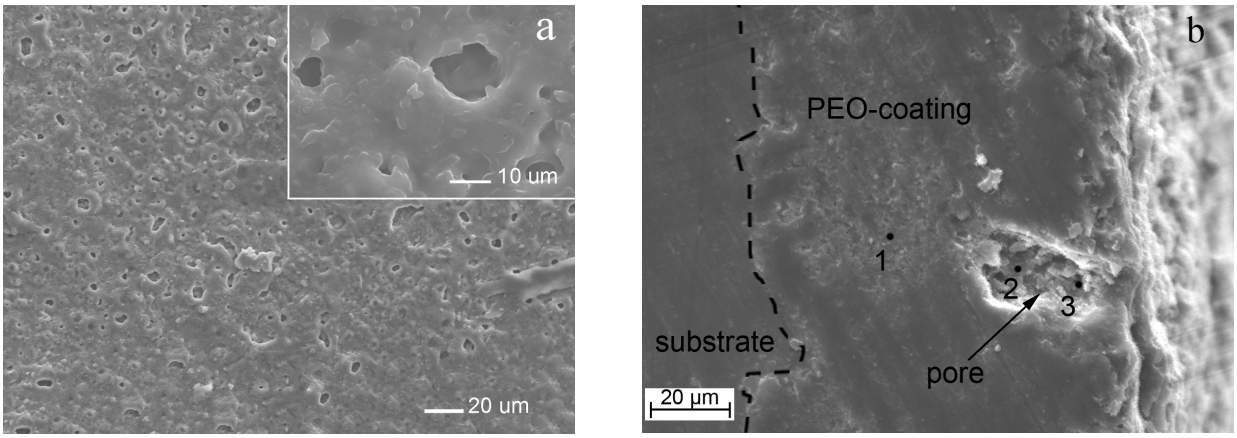


(a) (b)

**Fig. 4 SEM-images of the magnesium sample with PEO-coating after filling of pores with SPTFE: (a) surface and (b) cross-section observations.**

out, perturbing sinusoidal signals with an amplitude of 10 mV and a frequency varying from 0.005 Hz to 1 MHz with 10 points per decade were applied.

Potentiodynamic polarization curves recorded for the studied specimens are shown in Fig. 2a and the EIS results are presented in Fig. 2b in the Bode plots (impedance modulus $|Z|$ and phase angle θ versus the frequency $f$). Parameters of corrosion resistance derived from these plots are listed in Table 2. Analysis of the data in Table 2 allows claiming that the PEO coatings considerably reduce the dissolution rate of magnesium in the active region. Some quantitative difference of $|Z|_{f\to 0\ \mathrm{Hz}}$ and $R_p$ values shown in Table 2 links to the polarisation conditions of the sample under investigation used at potentiondynamic polarisation and impedance measurements. The impedance spectrum of the PEO coated specimen in the frequency range of $10^2$ to $10^6$ Hz has a complex character, which is probably due to the convoluted surface morphology (Fig. 2). The impedance modulus at low frequencies, which characterises the coating protective properties is $|Z|_{f\to 0\ Hz} = 5.07\cdot10^4\ \Omega\cdot cm^2$. This value is by more than 60 times higher than that for the uncoated sample ($|Z|_{f\to 0\ \mathrm{Hz}} = 8.09\cdot10^2\ \Omega\cdot cm^2$).

Results of corrosion evaluation in Hank's balanced salt solution at 37 ºC conducted using potentiodynamic polarization and EIS techniques are presented in Fig. 3a and 3b, c, d respectively. Polarization resistance, $R_P$, calculated from these measurements are presented in Table 3. Since the magnesium alloy substrate possesses a higher stability in the Hank's solution (which has a lower concentration of chloride ions) even at 37 ºC than in the 3% NaCl solution at 20 ºC (Table 2 and Table 3), the corrosion resistance of the PEO-coated alloy is not significantly affected by the physiological medium (Table 3).

To further improve the corrosion protection of the Mg alloy, the SPTFE post-treatment of the PEO-coating was applied, followed by the heat treatment. The SPTFE (trade mark Forum®) unlike PTFE is the convenient material for the formation of composite coatings due to its properties. This material contains a low-molecular fractions, which have the softening and melting temperatures lower than ones for PTFE. According to thermal analysis data the melting beginning of SPTFE is equal to about 220 °C. So, it provides the penetration of SPTFE into the pores of PEO-layer. This particular post-treatment procedure allows sealing predominantly the pores and cracks (Fig. 4a, b) [23,25]. The comparison of surface SEM images of the PEO-coatings before (Fig. 1a) and after SPTFE treatment (Fig. 4a) indicates about smoothing of the surface morphology as a result of the SPTFE post-treatment.

From EDS analysis the fluorine is predominantly distributed in the porous part of the coating (Fig. 4b). Thus the fluorine content in points 2 and 3 is equal to 23 and 36 at% respectively, which is considerably higher than that in the point 1 (about 8 at%). According to the data of Table 3, such post-treatment significantly reduces the corrosion current density (> 3 orders of magnitude) and, therefore, substantially (by about 3 orders of magnitude) increases both polarisation resistance and impedance modulus.

The graphs of the dependence of the impedance modulus on frequency (Fig. 2b and Fig. 3b) corroborate the conclusions based on the analysis of polarization curves. The values of the impedance modulus measured at low frequency ($|Z|_{f\to 0\mathrm{Hz}}$, Table 3) for the samples with a polymer layer on the surface are by more than one order of magnitude higher than those for the PEO-coating not treated with polymer and for the bare substrate as well. The

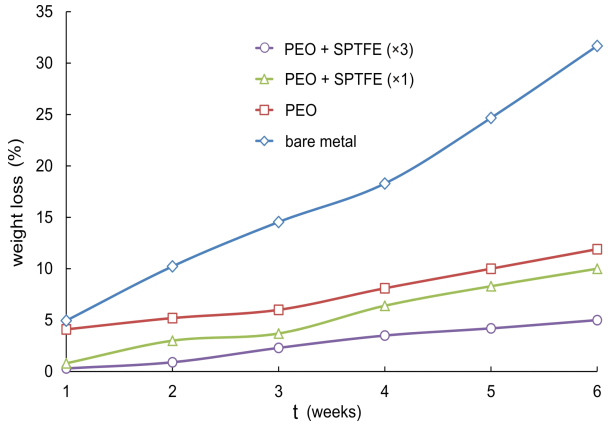


**Fig. 5 Evolution of weight loss of the magnesium samples with different surface treatment.**

dependence of the phase angle $\theta$ on frequency (Fig. 2b and Fig. 3b) reflects the changes in morphological properties and heterogeneity of samples during the formation of different composite layers on their surface. The impedance spectrum of a bare metal has one time constant i.e. one bend on the dependence of the phase angle θ on frequency (Fig. 2b and Fig. 3b).

The spectrum of a PEO-coating contains a two time constants. The first one characterizing the geometric capacity of the whole oxide layer, with the phase angle maximum –45°, is located in the frequency range between $1\cdot10^3$–$1\cdot10^5$ Hz. The more expressed second time constant responsible for the nonporous sublayer, with the phase angle maximum –50°, is located in the frequency range between $10^{-2}$–$10^2$ Hz. This spectrum is fitted, with high accuracy ($\chi^2 = 1.2\cdot10^{-4}$), by an equivalent electrical circuit consisting of a parallel connection of two *R*–*CPE*-circuits, in which the $R_1$ and $CPE_1$ elements describe the porous part of the oxide layer, whereas the $R_2$ and $CPE_2$ elements are related to the poreless sublayer. The *CPE* impedance is determined in accordance with the equation: $Z_{CPE} = 1/[Y_o(j\omega)^n]$, where $\omega$ is an angular frequency ($\omega = 2\pi f$), $j$ is an imaginary unit, $n$ and $Y_o$ are the exponential coefficient and the frequency independent constant, respectively [17–20]. The composite layer formed as a result of treatment of the PEO-coating with SPTFE can be again characterize by equivalent electrical circuit with one time constant (Fig. 3b, d). Therefore, the porous part is really filled with polymer and the composite layer on the dependence of the phase angle $\theta$ on frequency looks like as poreless. High value of the phase angle in the maximum of dependence about –90° testifies to capacitive behavior of composite layer.

The degradation rates of MA8 alloy samples with a different surface treatment at exposure during 6 week to SBF solution were investigated. The weight loss was determined by volumetry method from the volume of the hydrogen evolution during the corrosion process. In accordance with the resulting corrosion reaction of Mg, one molecule of hydrogen is evolved as a result of each atom oxidation of corroded Mg. One mol (i.e. 24.31 g) of Mg metal corrodes for each mol (i.e. 22.4 l) of hydrogen gas produced. Therefore, the hydrogen evolution rate, $V_H$ (ml/cm$^2$/day), is related to the metal weight loss rate, $\Delta W$ (mg/cm$^2$/day), according to equation: $\Delta W = 1.085\times V_H$. As shown in Fig. 5 the sample with composite coating obtained by PEO and subsequent triple SPTFE treatment has a lowest mass loss (5 %). Therefore, the corrosion rate for this sample is more than 3-fold and 6-fold lower than that of the samples with PEO-coating and bare substrate, respectively.

Thus, the hydroxyapatite based PEO-coatings followed by SPTEF treatment substantially reduce corrosion rate of the magnesium alloy substrate. The original method developed for surface treatment of Mg alloys has significant potential for application to biodegradable magnesium implants, which could bring the implant surgery to a qualitatively new level.

### 2.2. Anticorrosive titanium nickelide based coatings

Nowadays very little information about the protective coatings on titanium nickelide (unlike titanium and aluminum alloys) and especially about the surface treatment by the PEO method can be found in the literature. Only few papers of other authors in which used the PEO method for formation coating on NiTi alloys have been published [26–31].

As a result of our search devoted to the formation of protective surface layers, the electrolyte containing sodium aluminate ($NaAlO_2$), sodium carbonate ($Na_2CO_3$), and three-substituted sodium phosphate ($Na_3PO_4\cdot12H_2O$) was chosen. Based on the principles of directed plasma-electrolysis synthesis developed in [32] it was assumed that titanium layers containing aluminum compounds (oxides and phosphates) and titanium dioxide ($TiO_2$) can be formed in the given electrolyte on the titanium nickelide surface. In addition, dimethylglyoxime (DMGO), which bounds nickel ions $Ni^{2+}$ into chelate compounds (nickel dimethylglyoximate $Ni(HC_4H_6N_2O_2)_2$ having red color) was added to the electrolyte. It was assumed that nickel cations ($Ni^{2+}$) formed in the electrolyte solution in the process of oxidation during anode dissolution of nickel from titanium nickelide, will be bound by dimethylglyoxime into complex compounds stable at room temperature and insoluble in aqueous electrolyte. According to the suggested mechanism, the deposit of this complex will

reduce the porosity of the newly formed layer, increasing its corrosive properties. The presence of nickel dimethylglyoximate in the electrolyte solution is testified by the painted deposit arising in the oxidation process both in the volume of the electrolytic bath and at the surface of the sample being oxidized.

According to X-ray diffraction (XRD) data [21], aluminum phosphate ($AlPO_4$) and nickel-aluminum oxide ($NiAl_2O_4$) were comprised in the coating. An analysis of diffraction patterns of the surface layers of some samples established the presence of oxygen-containing nickel and titanium compounds ($Ni_3Ti_3O$) whose concentrations were small. At the same time, no titanium oxides were revealed in the surface layers. Fig. 6 shows an optical photograph of the cross-section of the sample with PEO-coating on the surface. The thickness of the PEO-coating was equal to about 20 μm. An analysis of the photograph demonstrated that the surface of the layers formed on titanium was inhomogeneous: pores and roughness can be seen. It seemed likely that coatings have a cluster's morphology.

Since the state of the product surface influences significantly on its behavior in a corrosion-active medium [33], to change the state of the surface of the initial material and to reveal subsequently the influence of this change, titanium nickelide samples were treated by several methods:

1) Deposition on the surface of SPTFE followed by heating treatment at 100 °C for 1 h.

2) Plasma electrolytic oxidation in the potentiodynamic unipolar mode up to 180 V with voltage sweep rate of 0.25 V/s and in the sign-alternating bipolar regime. The bipolar regime represented a combination of the anode potentiostatic ($dU/dt$ = 0.25 V/s) and cathode galvanostatic ($j_c$ = 0.5 A/cm$^2$) polarization. The anode and cathode polarization periods were in the ratio $\tau_a/\tau_c$ = 4.

3) Plasma electrolytic oxidation (in the mode corresponding to item 2) with subsequent deposition of SPTFE on the PEO layer surface and followed by heating treatment at 100 °C for 1 h.

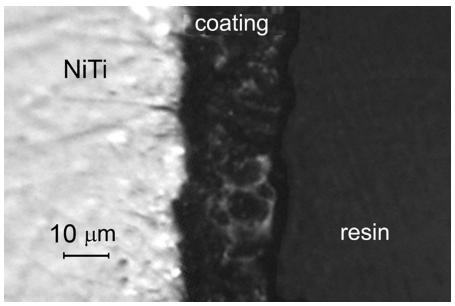


**Fig. 6 Cross-section of the PEO-coating formed on the titanium nickelide surface [18].**

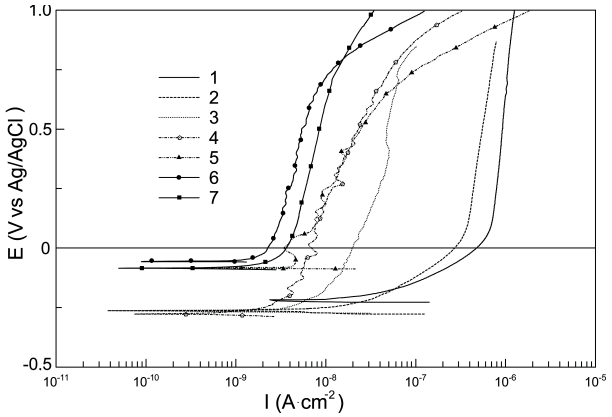


**Fig. 7 Polarization curves in the physiological solution recorded with sweep rate v = 10 mV/min. Notation of the samples is given in the Table 4.**

The electrochemical properties of layers formed on nitinol were investigated by potentiodynamic polarization and electrochemical impedance spectroscopy with using the electrochemical system 12558WB (Solartron Analytical, UK). The measurements were carried out in three electrode cells at room temperature in an artificial physiological solution (NaCl – 8.4 g/l; $NaHCO_3$ – 0.35 g/l; $Na_2HPO_4 \cdot 2H_2O$ – 0.06 g/l; $NaH_2PO_4 \cdot 2H_2O$ – 0.06 g/l). Platinized niobium grid was used as a counter electrode. The silver/silver chloride electrode filled with saturated solution of KCl was used as a reference electrode. The exposition area of the working electrode was equal to 0.72 cm$^2$. The experiment management was performed with using the software CorrWare/ZPlot (Scribner Associates, Inc.). The impedance spectra were recorded at open circuit potential. The sine-wave signal with the amplitude 10 mV was used as an excitation signal.

An analysis of the electrochemical behavior of samples in the physiological solution (Fig. 7) demonstrated that the maximum protective properties possessed composite coatings with the PEO layer treated with SPTFE (curves *6* and *7* in Fig. 7). Such treatment led to ennoblement of the free corrosion potential ($E_C$) of the sample and to the decrease in the corrosion currents ($I_C$).

Incorporation of dimethylglyoxime into the forming solution also entailed a small impove in the protective properties (this conclusion was made based on a comparison of samples # 3 and # 5). Table 4 presents comparative corrosion characteristics of the titanium nickelide samples treated by different methods. The value of the polarization resistance ($R_P$) of the sample evaluated from the linear section of the polarization curve in the field of free corrosion potential is also presented in the Table 4.

**Table 4 Corrosion properties of the examined titanium nickelide samples with different coatings [21]**

| Sample # | Regime of coating formation | $E_C$ (V vs Ag/AgCl) | $I_C$ (A/cm$^2$) | $R_P$ ($\Omega$·cm$^2$) |
|---|---|---|---|---|
| 1 | Without coating | –0.22 | $1.7\cdot10^{-7}$ | $1.6\cdot10^{5}$ |
| 2 | SPTFE (heating treatment at 100 °C for 1 h) | –0.26 | $1.1\cdot10^{-7}$ | $2.3\cdot10^{5}$ |
| 3 | PEO in the unipolar mode, electrolyte: $Na_3PO_4\cdot12H_2O$ – 10 g/l $NaAlO_2$ – 20 g/l, $Na_2CO_3$ – 10 g/l | –0.26 | $4.1\cdot10^{-8}$ | $6.5\cdot10^{5}$ |
| 4 | PEO in the bipolar mode, electrolyte: $Na_3PO_4\cdot12H_2O$ – 10 g/l, $NaAlO_2$ – 20 g/l, $Na_2CO_3$ – 10 g/l | –0.27 | $4.0\cdot10^{-9}$ | $6.6\cdot10^{6}$ |
| 5 | PEO in the unipolar mode, electrolyte: $Na_3PO_4\cdot12H_2O$ – 10 g/l, $NaAlO_2$ – 20 g/l, $Na_2CO_3$ – 10 g/l, DMGO – 1 g/l | –0.08 | $2.3\cdot10^{-8}$ | $8.1\cdot10^{5}$ |
| 6 | As sample # 3 + SPTFE | –0.06 | $4.3\cdot10^{-9}$ | $6.1\cdot10^{6}$ |
| 7 | As sample # 4 + SPTFE | –0.08 | $3.7\cdot10^{-9}$ | $9.1\cdot10^{6}$ |

An analysis of the results of electrochemical investigations [21] demonstrated that the surface treatment of titanium nickelide by superdispersed polytetrafluoroethylene influenced slightly the state of the electrode/electrolyte interface, reducing the anode current only insignificantly (Fig. 7). The weak effect of such treatment is most likely due to poor adhesion of the polymer to the metal substrate and insufficient continuity of the formed protective layer. Treatment of the sample by the PEO method increased its stability in the examined medium [34]. Addition of dimethylglyoxime into the electrolyte increased the protective properties of coatings (curve *5* in Fig. 7); however, the difference is very little. The significant increase of only the free corrosion potential can be seen on the polarization curves (curve *5* in Fig. 7). The anode current for such coating, commensurable in the initial section with the anode current for the sample with the PEO layer formed in the bipolar mode, after 0.7 V becomes even greater than for other samples with PEO-coatings. This suggests that the chelate nickel dimethylglyoximate compound, being deposited into pores of the oxide layer, leads to a certain imrove in the protective properties of the surface layer. However, its concentration in the film is not high (less than 10 %), since no reflections corresponding to this phase were fixed on the diffraction pattern. Being a thermally unstable compound [35,46], nickel dimethylglyoximate partially decomposes during plasma electrolysis, which is accompanied, as it is well known, by high temperatures realized in short-living plasma channels, as well as during thermolysis in coating regions adjacent to the plasma channel. Thus, the low content of nickel dimethylgluoximate in the coating pores does not allow significant corrosion protection to be provided at large anodic biases.

It should be taken into account that the PEO-coating represents the layer consisting of the outer – porous sublayer and inner – poreless sublayer. The porous intermediate layer, as a rule, has crater-like cavities with a diameter up to several microns. Thus, the pore sizes are somewhat greater than sizes of SPTFE powder particles (about 1 μm) used for film surface treatment. The formation of the porous structure of the surface can be the additional advantage of the PEO method, since the bone tissue grows better on the rough surface of the implant, thereby filling the pores with bioinert or bioactive composites. After treatment of the sample with PEO-coating with SPTFE, the impedance modulus significantly increased and becomes by 10 fold higher than for the sample without coating [40]. This demonstrates that treatment by SPTFE allows the coating pores to be filled with polymer and the additional barrier layer preventing metal ion release into the solution to be created. This conclusion was confirmed by atomic absorption method. The concentration of nickel ions in the physiological SBF solution as a result of immersion in this media for 2 weeks at 37 °C of PEO + SPTFE pretreated NiTi samples has abated by one order of magnitude in comparison with bare (without treatment) titanium nickelide (Table 5).

Thus, the prospects for the application of the method of plasma electrolytic oxidation are demonstrated for the formation of coatings on the titanium nickelide surface improving its morphological structure and electrochemical properties. It was established that the application of superdispersed polytetrafluoroethylene as a part of the compo-

**Table 5 Concentration of nickel ions in the physiological solution (Simulated Body Fluid) as a result of immersion in this media for 2 weeks at 37 °C of NiTi samples after different surface treatment**

| Kind of surface treatment | Ni concentration (μg/ml) |
|---|---|
| bare NiTi | 0.055 |
| NiTi + PEO | 0.019 |
| NiTi + PEO + SPTFE | 0.006 |
| SBF solution (due to impurities) | 0.004 |

site coating on the given material allows increasing its stability in a corrosion-active medium [31]. The combined action of polarization and plasma on the sample surface during PEO allows forming the coatings with protective anticorrosive properties. Such layers contain pores in the surface part of the coating that can be used as a container for the medicine (for example, antibiotics, hydroxyapatite, or other phosphate-containing substances providing the best compatibility with bone tissues if one needs to obtain a biologically-active implant surface or polymer powder if one needs to obtain a biologically inert surface). As demonstrated experimentally [31,36], after filling of pores with superdispersed polytetrafluoroethylene powder which can be used as a polymer, thermal treatment is required to obtain smoothed hydrophobic surface layers. In this case, the polymer fills pores into which the medicine can be preliminary injected and thus their diffusion from the surface layers can be reduced. This increased the duration of therapeutic effect of the medicine comprised in the pore. In addition, the anticorrosive coating being formed considerably reduced diffusion of nickel ions from titanium nickelide and hindered their accumulation in human tissues [21].

## 3. Conclusions

This work has experimentally demonstrated that hydroxyapatite-containing protective coatings with the Ca/P ratio close to that of the bone tissue can be fabricated on the surface of Mg-Mn-Ce alloy by the pulsed bipolar PEO process in the electrolyte containing calcium glycerophosphate and sodium fluoride. The coatings have a convoluted porous morphology, which is favourable for osteoblast adhesion, and, at the same time, significantly reduces the corrosion rate of the magnesium alloy, which allows them to be considered promising for biodegradable Mg implant applications. Additional sealing of the porous part of the coating with SPTFE powder significantly improves the corrosion protectin of magnesium implant in physiological solution. The corrosion resistant layers formed using plasma electrolytic oxidation with subsequent SPTFE-treatment on the surface of titanium nickelide have been developed. The results of the comprehensive study show improvement of the protective characteristics and significant reduction of the nickel ions diffusion.

## Acknowledgments

This work was supported by the Grant of Russian Science Foundation (project №14-33-00009).

## References

1. M. P. Staiger, A. M. Pietak, J. Huadmai, and G. Dias, *Biomaterals*, **27**, 1728 (2006).
2. F. Witte, N. Hort, C. Vogt, S. Cohen, K. U. Kaine, R. Willumeit, and F. Feyerabend, *Curr. Opin. Solid St. M.*, **12**, 63 (2008).
3. F. Witte, *Acta Biomater.*, **6**, 1680 (2010).
4. R. C. Zeng, W. Dietzel, F. Witte, N. Hort, and C. Blawert, *Adv. Eng. Mater.*, **10**, B3 (2008).
5. M. Carboneras, M. C. Garcia-Alonso, and M. L. Escudero, *Corros. Sci.*, **53**, 1433 (2011).
6. A. Purnama, H. Hermawan, J. Couet, and D. Mantovani, *Acta Biomater.*, **6**, 1800 (2010).
7. X. N. Gu and Y. F. Zheng, *Front. Mater. Sci. China*, **4**, 111 (2010).
8. S. Hiromoto, T. Shishido, A. Yamamoto, N. Maruyama, H. Somekawa, and T. Mukai, *Corros. Sci.*, **50,** 2906 (2008).
9. K. C. W. Wu, Y. H. Yang, Y. H Liang, H. Y. Chen, E. Sung, Y. Yamauchi, and H. L. Feng, *Curr. Nanosci.*, **7**, 926 (2011).
10. B. P. Bastakoti, M. Inuoe, S. Yusa, S. H. Liao, K. C. Wu, K. Nakashima, and Y. Yamauchi, *Chem. Commun.*, **48**, 6532 (2012).
11. Y. T. Huang, M. Imura, Y. Nemoto, C. H. Cheng, and Y. Yamauchi, *Sci. Technol. Adv. Mat.*, **12,** 045005 (2011).
12. L. Tan, Q. Wang, F. Geng, X. Xi, J. Qiu, and K. Yang, *Trans. Nonferrous Met. Soc. China*, **20**, 648 (2010).
13. D. Lee, Ch. Sfeir, and P. Kuneta, *Mater. Sci. Eng. C.*, **29**, 69 (2009).
14. M. Tomozawa, S. Hiromoto, and H. Yoshimoto, *Surf. Coat. Technol.*, **204**, 3243 (2010).
15. Kusukawa Kazuhiro, Biological material and method of manufacturing the same, 2007–202782. (2007.08.16).
16. S. V. Gnedenkov, O. A. Khrisanfova, S. L. Sinebryukhov, A. V. Puz', and M. V. Sidorova, Method of the calcium -phosphate coating of titanium and titanium alloys implants, 2348744 (2009.03.10).

17. S. V. Gnedenkov, Yu. P. Scharkeev, S. L. Sinebryukhov, O. A. Khrisanfova, E. V. Legostaeva, A. G. Zavidnaya, A. V. Puz', and I. A. Khlusov, *Inorg. Mater. Appl. Res.*, **2**, 474 (2011).
18. Zh. Yao, L. Li, and Zh. Jiang, *Appl. Surf. Sci.*, **255**, 6724 (2009).
19. P. B. Shrinivasan, J. Liang, C. Blawert, M. Störmer, and W. Dietzel, *Appl. Surf. Sci.*, 256 4017–4022 (2010).
20. S. V. Gnedenkov, O. A. Khrisanfova, A. G. Zavidnaya, S. L. Sinebryukhov, V. S. Egorkin, M. V. Nistratova, A. Yerokhin, and A. Matthews, *Surf. Coat. Technol.*, **204**, 2316 (2010).
21. S. V. Gnedenkov and S. L Sinebryukhov, *Compos. Interface.*, **16**, 387 (2009).
22. S. V. Gnedenkov, O. A. Khrisanfova, and A. G Zavidnaya, *Plasma electrolytic oxidation of metals and alloys in tartrate-containing solutions*. Dal'nauka, Vladivostok, Russian (2008).
23. S. V. Gnedenkov, S. L. Sinebryukhov, and V. I. Sergienko, *Composite multifunctional coatings formed on the metals and alloys by plasma electrolytic oxidation*, p. 460, Dal'nauka, Vladivostok, Russian (2013).
24. P. Sun, Y. Lu, Y. Yuan, X. Jing, and M. Zhang, *Surf. Coat. Technol.*, **205**, 4500 (2011).
25. A. N. Minaev, S. V. Gnedenkov, S. L. Sinebryukhov, D. V. Mashtalyar, M. V. Sidorova, Yu. V. Tsvetkov, and A. V. Samokhin, *Protect. Met.*, **47**, 840 (2011).
26. H. T. Siu and H. C. Man, *Appl. Surf. Sci.*, **274,** 181 (2013).
27. J. L. Xu, F. Liu, D. Z. Yu, and L. C. Zhao, Curr. Appl. Phys., **9,** 663 (2009).
28. J. L. Xu, F. Liu, F. P. Wang, and L. C. Zhao, *Mater. Lett.*, **62**, 4112 (2008).
29. J. L. Xu, F. Liu, F. P. Wang, D. Z. Yu, and L. C. Zhao, *Appl. Surf. Sci.*, **254,** 6642 (2008).
30. F. Liu, J. Xu, F. Wang, L. Zhao, and T. Shimizu, *Surf. Coat. Technol.*, **204,** 3294 (2010).
31. H. Wang, F. Liu, Y. Zhang, and F. Wang, *Surf. Coat. Technol.*, **206**, 4054 (2012).
32. O. A. Khrisanphova, L. M. Volkova, S. V. Gnedenkov, T. A. Kaydalova, and P. S. Gordienko, *Zh. Neorg. Khim.*, **40**, 558 (1995).
33. G. Rondelli, *Biomaterials*, **17**, 2003 (1996).
34. S. V. Gnedenkov, S. L. Sinebryukhov, D. V. Mashtalyar, V. S. Egorkin, A. K. Tsvetnikov, and A. N. Minaev, *Protect. Met.*, **44**, 704 (2008).
35. X. Li, X. Zhang, Z. Li, and Y. Qian, *Solid State Commun.*, **137**, 581 (2006).
36. S. L. Sinebryukhov, A. S. Gnedenkov, O. A. Khrisanphova, and S. V. Gnedenkov, *Surf. Eng.*, **25**, 565 (2009).